MECHANIKA
TEORETYCZNA
I STOSOWANA
2, 26 (1988)

SPECKLE PATTERN CORRELATION USING DIGITAL IMAGE PROCESSING*

ROLAND HÖFLING
WOLFGANG OSTEN

Academy of Sciences of GDR — Karl-Marx-Stadt and Berlin

1. Introduction

Over the last 15 years, a lot of work has been done in the field of displacement measurement by coherent optics. One of the methods, beside holographic interferometry, is speckle metrology which splits into Speckle Pattern Photography (SPP) and Speckle Pattern Interferometry (SPI). Depending on the point of view, the measurement principle has been described in different terms by several authors and the sum of literature is not always easy to be understood. SPP is sometimes explained by moire terminology and the basic relations in SPI originate from optical path length argumentations similar to holographic interferometry. In basic papers by Pedersen and Yamagushi [1, 2] speckle metrology is explained from a unified point of view: intensity correlation.

In section 2 we follow this theory in order to explain the measuring principle of Digital Speckle Pattern Interferometry (DSPI) and give a simulation example of it. The experimental arrangement incorporating a digital image processing system Robotron A6472 is discussed in section 3. The online data pickup and correlogram construction enable us to proceed with automatic evaluation which is subject to chapter 4.

2. Speckle pattern interferometry — an intensity correlation technique

The basic relation in speckle pattern correlation measurements connects the crosscorrelation function with the mutual intensity of the light field scattered from the undeformed ($j = 1$) and deformed ($j = 2$) object, respectively:

$$\sigma_{12} = \frac{\langle \Delta I_1 \Delta I_2 \rangle}{\langle I_1 \rangle \langle I_2 \rangle} = \frac{|\langle U_1^* U_2 \rangle|^2}{\langle I_1 \rangle \langle I_2 \rangle} \tag{1}$$

and holds if the speckle pattern obeys gaussian statistics (3). I_j and U_j denote the intensity and amplitude field of the light and $\langle \ldots \rangle$ is an ensemble mean. In the following, we consider SPI only and assume the speckle position to be fixed, i.e. no speckle shift. Beyond

* Praca wygłoszona na XII Sympozjum Doświadczalnych Badań w Mechanice Ciała Stałego Warszawa-Jadwisin, 1986.

this, the mean intensities $\langle I_1 \rangle$ and $\langle I_2 \rangle$ should be equal, thus we drop the index. The mutual intensity in this case becomes:

$$\langle U_1^* U_2 \rangle = \langle I \rangle \exp\left(\frac{2\pi}{\lambda} \mathrm{i}(\boldsymbol{h}-\boldsymbol{k})\boldsymbol{d}\right), \tag{2}$$

where $\boldsymbol{h}$ and $\boldsymbol{k}$ are the unit vectors of the illumination any observation direction, respectively. $\boldsymbol{d} = (d_1, d_2, d_3)^T$ denotes the displacement vector field and λ is the wavelength of the used laser light. As it is obvious from Eq. (2) the correlation function of a simple illuminated and observed object is a constant. In common SPI setups, two statistically independent speckle patterns U^1 and U^2 are superposed in order to produce interferometric sensitivity [4]. We than have:

$$\langle U_1^* U_2 \rangle = \langle U_1^{1*} U_2^1 \rangle + \langle U_1^{2*} U_2^2 \rangle, \tag{3}$$

and with (1) and (2):

$$\varrho_{12} = \frac{\langle I^1 \rangle^2 + \langle I^2 \rangle^2 + 2\langle I^1 \rangle \langle I^2 \rangle \cos\left(\frac{2\pi}{\lambda}(\boldsymbol{h}_1 - \boldsymbol{h}_2 - (\boldsymbol{k}_1 - \boldsymbol{k}_2)) \cdot \boldsymbol{d}\right)}{(\langle I^1 \rangle + \langle I^2 \rangle)^2}. \tag{4}$$

Before we apply Eq. (4) to given interferograms, we select the case of maximal contrast of correlation fringes. This is achieved, if the mean intensities of the interfering speckle fields are equal: $\langle I^1 \rangle = \langle I^2 \rangle$. With the abbreviation $\boldsymbol{S}$ for the sensitivity vector we finally get:

$$\varrho_{12} = \frac{1}{2}\left(1 + \cos\left(\frac{2\pi}{\lambda} \boldsymbol{S} \cdot \boldsymbol{d}\right)\right), \tag{5}$$

$$\boldsymbol{S} = (\boldsymbol{h}_1 - \boldsymbol{k}_1) - (\boldsymbol{h}_2 - \boldsymbol{k}_2). \tag{6}$$

With the proper choice of illumination and observation geometries the sensitivity vector $\boldsymbol{S}$ allows to separate displacement components lying both in the object surface tangential plane and normal to it.

2.1. In-plane sensitivity. The scheme of an interferometer capable of in-plane displacement measurements [4] is plotted in figure 1. The object is illuminated by two collimated beams in a symmetric manner. Both beams create independent speckle patterns that inter-

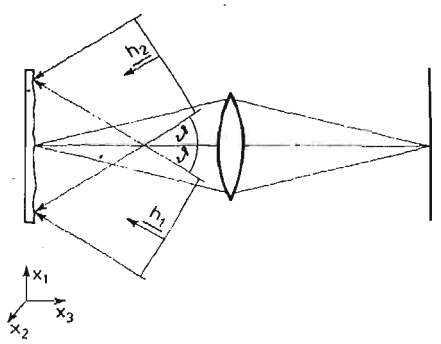

Fig. 1. Double-beam interferometr for in-plane displacement measurements

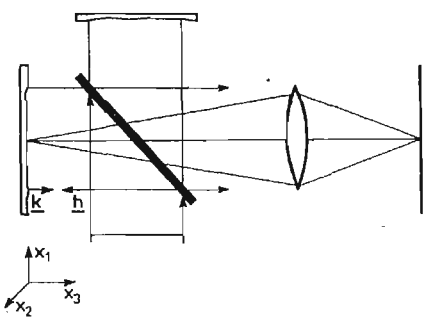

Fig. 2. Modified Michelson interferometr for out-of plane displacement measurements

fere on the detector plane and produce a resulting third pattern. Assuming parralel observation for the field of view Eq. (6) yields:

$$\boldsymbol{S} = \sin\vartheta(1, 0, 0)^{\mathrm{T}} \tag{7}$$

and reveals independence of out-of plane displacements. This is a very important distinction to holographic interferometry. From the spacing of correlation fringes strain may be obtained directly without solving systems of equations and without knowledge of the absolute fringe orders.

2.2. Out-of plane sensitivity. There are different interferometric setups realizing out-of plane displacement measurements [4]. A common method is the superposition of a smooth reference wave with its virtual source at the centre of the imaging aperture. We describe two other arrangements less complicated in adjustment. The first is shown in figure 2 and consists in a modified Michelson interferometer. The mirrors have been substituted by diffus scattering object and reference surfaces. They are illuminated by the beam splitter. mirror and the reflected speckle fields are collected again to interfere. The sensitivity vector becomes:

$$\boldsymbol{S} = (0, 0, 2)^{\mathrm{T}}. \tag{8}$$

In practical applications the sensitivity according to Equ. (8) may be too high and therefore an interferometer of reduced sensitivity has been developed [4]. It is sketched in figure 3.

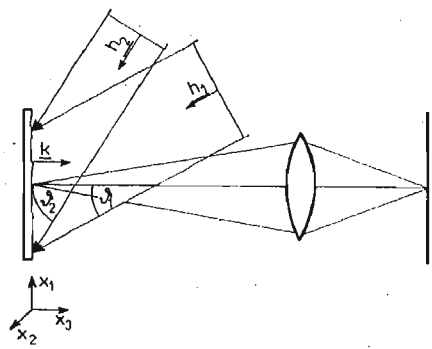

Fig. 3. Interferometr with reduced out-of plane sensitivity

The sensitivity vector is:

$$\boldsymbol{S} = (\sin\vartheta_1 - \sin\vartheta_2, 0, \cos\vartheta_1 - \cos\vartheta_2)^{\mathrm{T}}, \tag{9}$$

and in the limit of streaking illumination $\left(\vartheta_1, \vartheta_2 \to \frac{\pi}{2}\right)$ we have:

$$\boldsymbol{S} = (0, 0, \vartheta_2 - \vartheta_1)^{\mathrm{T}}. \tag{10}$$

3. Correlogram formation in speckle pattern interferometry

In section 2 it is shown which relations exist between the displacement vector field $\boldsymbol{d}$ and the crosscorrelation function. The remaining question is, how to measure that quantity. Different methods have been developed from several authors and fall into two cathegories: optical and electronical. In optical processing the speckle fields of both object

states are recorded on the same photographic plate. Sharp structures of the speckle pattern itself or additional introduced speckle structuring (interference or shift) are exploited to detect regions of decorrelation (i.e. vanishing structures) by an optical Fourierprocessing.

Electronic processing allows to bypass the photochemical process by pattern recording with photoelectric detectors (TV pickup tube, CCD matrix, photodiode array) thereby simplifying the procedure and making it more acceptable for application. The method is called Electronic Speckle Pattern Interferometry (ESPI). ESPI is a widely used tool in vibration mode and displacement visualization for scientific and engineering purpose [5, 6]. Visual fringe interpretation, however, often yields qualitative results only.

The reduced volume and cost of memory circuits recommend the video recording media used in ESPI to be substituted by more accurate digital image memories. Consequently, a computer may be used to perform both correlation of the stored speckle patterns and displacement extraction from the resulting correlograms (often called "interferograms"). Some recent papers [7 - 11] present this Digital Speckle Pattern Interferometry (DSPI) and introduce phase shifting techniques in order to get quantitative results. Digital pattern processing by today's microcomputer systems suffers from high processing time requirements for full TV image operations (e.g. 512×512 pixel). Offline links to large scale computers [7] or reduced pixel numbers [8 - 11] are reported relaxing the time problem. We, instead, use the fast pipeline image processor that realizes image opertions at video rates (40 ms) by virtue of the SIMD principle. It provides real-time correlograms as well as fast online evaluation.

The way of getting the desired correlation function depends on the type of experiments: dynamic or static load. In the case of dynamic loads (vibration, shock) the patterns are added in the photodetector already either in a time-average or a double exposition fashion. The speckle contrast of the resulting pattern is related to the degree of correlation and high pass filters or level-windowing techniques convert contrast variations into brightness fringes.

We focus our interest on the static load case and investigate what happens in detaile. The patterns of the initial and deformed state of the object are recorded successively and stored on a video tape or in a digital memory. After that, the squared difference of the patterns I_1 and I_2 is displayed. If we replace the ensemble mean by a spatial average (i.e.

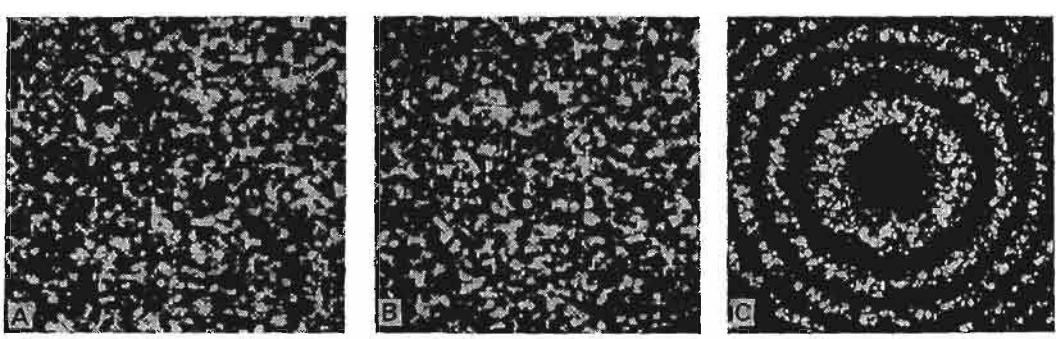

Fig. 4. Example correlogram formation
(A) pattern of the underformed state, (B) pattern of the deformed state, (C) squared difference $(A - B)^2$

by eye), we measure:

$$\langle (I_1 - I_2)^2 \rangle = 2\langle I \rangle^2 (1 - \varrho_{12}) \tag{11}$$

and from Eq. (5) we get:

$$\langle (I_1 - I_2)^2 \rangle = 2\langle I \rangle^2 \sin^2 \left(\frac{2\pi}{\lambda} \boldsymbol{S} \cdot \boldsymbol{d} \right). \tag{12}$$

In order to give an example, figure 4 shows the monitor print of two different simulated speckle patterns [12] whose mutual correlation is $\varrho_{12} \sim (k-k_0)^2 + (l-l_0)^2$ where (k_0, l_0) denotes pixel locations in the image center. Clear correlation fringes are visible is the patterns are subtracted and squared according to Eq. (11).

4. Experimental results in DSPI

The scheme of our speckle pattern interferometer is drawn in figure 5. The expanded and collimated light from a 30 mW He-Ne laser is directed to a beam splitter mirror thus illuminating a 50 mm-spot on the diffusely scattering reference and object surfaces. One of the objects is a central loaded circular disk, sprayed white. The reflected light of both surfaces is collected again by the mirror and imaged onto the pickup tube of a simple TV camera. A numerical apertur (NA) = 5.6 has been found sufficient for the camera

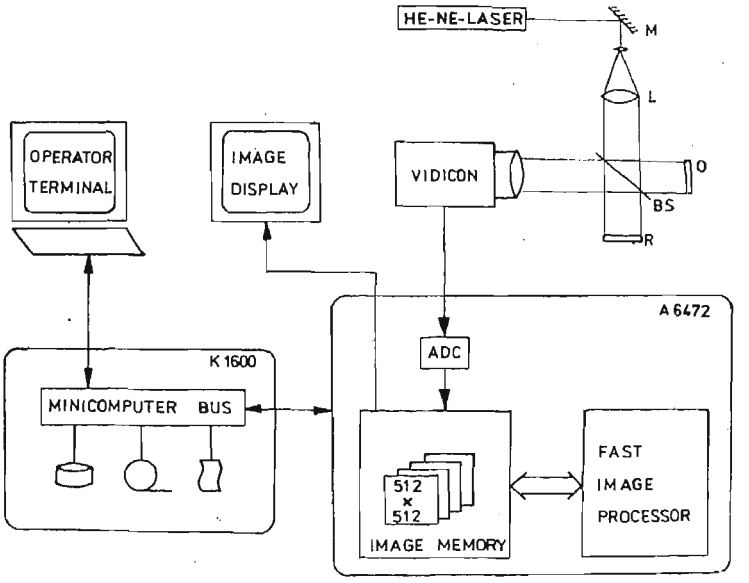

Fig. 5. Schematic diagram of the experimental setup

M ... mirror, *L* ... beam expanding lenses, *O* ... object, *R* ... reference surface, *BS* ... beam splitter

lens, although the resulting speckles (typically less than 15 μm in size) are not completely resolved by our vidicon. The camera signal is fed to the image processing system and digitized to be stored in one of the four 512 × 512 pixel image memories, each 8 bit deep. The squared and level sliced difference between a stored reference frame and the live

camera image is presented on the image display at video rates using the fast pipeline processor K2072 of the image processing system ROBOTRON A6472.
If only one TV frame is used for the reference pattern heavy electronic noise impairs the fringe contrast (figure 6(A)). According to its origin, electronic noise may be reduced drastically by frame averaging. Mostly we use 12 - 20 TV frames for at least the reference pattern. The frame averaging takes us about 2 seconds but produces much better correlograms almost free of electronic noise (figure 6(B)). Up to 50 straight or 18 closed circular fringes have been counted by eye. Sometimes the interferometer head has been changed (according to figure 1) in order to investigate in-plane deformations. Some results with different types of deformation are shown in figure 7.

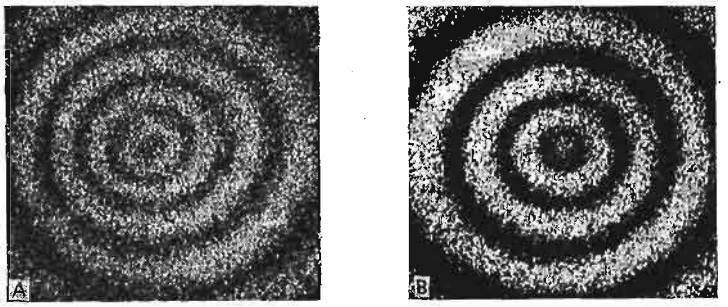

Fig. 6. Influence of frame averaging
(A) correlogram with high electronic noise (single frame), (B) correlogram from frame everaged speckle patterns

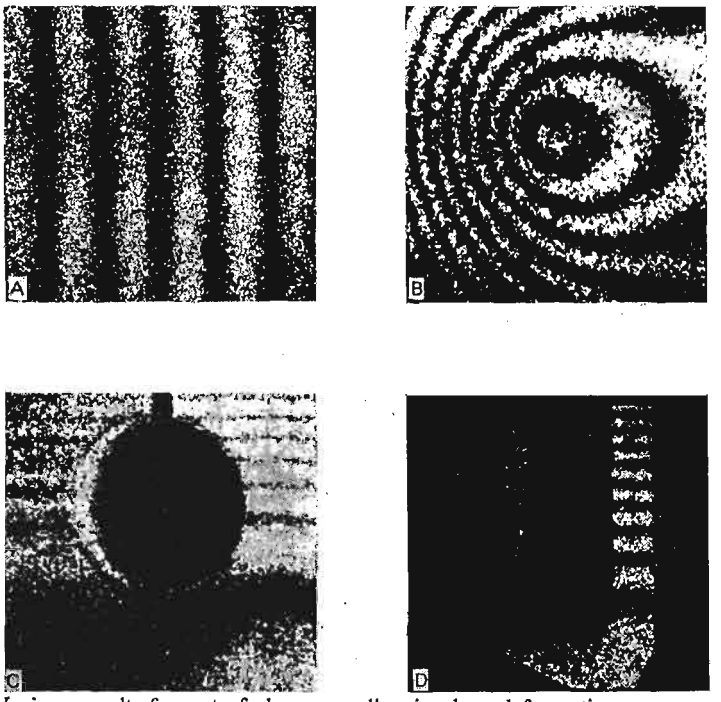

Fig. 7. Various results for out-of plane as well as in-plane deformation measurements
(A) pure out-of plane tilt, (B) combination of tilt and out-of plane deformation (as in fig. 6), (C) in-plane deformation of a clamp with a hole, (D) static in-plane deformation of a tuning-fork

5. Automatic evaluation of DSPI correlograms

From Eq. (12) it is obvious, that displacement extraction from a correlogram may take advantage from extrema locations that coincide with:

$$\boldsymbol{S} \cdot \boldsymbol{d} = N\frac{\lambda}{2}, \quad N = 0, 1, 2, \ldots \tag{13}$$

In order to get automatically all points satisfying Eq. (13) fringe centres (or skeletons) of the correlogram have to be found. Image processing software is available for this purpose in holographic interferometry [13, 14] and we apply it to DSPI correlograms. It is suggested sometimes that automatic fringe centre determination is hard if not impossible in speckle pattern interferometry. We found the line thinning algorithm working quite good if careful prepocessing has been applied to the correlogram.

5.1. Preprocessing of correlograms. Speckles carry the displacement information in DSPI but after the correlogram is obtained they represent pure noise. This is a main source of casual errors in DSPI [7] and some care should be taken of suppressing it. A common method is the application of mean filters (digital low-pass filters) which are simple and fast but they will fail in critical applications because of image blurring. Examples are shown in figure 7 where different window sizes have been used. Although speckles are not removed completely the fringes tend to fuse already. That for, a special geometric filter, proposed by Crimmins [15, 16] has been implemented and gives significant more clear fringes than mean filters do (figure 8) if the fringes are dense.

After correlogram smoothing a shading correction is recommended for equalization of fringe modulation. This is done, deviding the correlogram by the mean intensity $\langle I \rangle$ which may to obtained from camera again or be calculated from the correlogram by a large-window mean filter that causes the fringes to blur. After the equalization step a global threshold may be found for image binarization. Two examples are presented in figure 9.

5.2 Skeleton based evaluation. Binary fringes are the starting point for line thinning algorithms that produce a fringe skeleton (3 - 10 s) as it is visible in figure 10.
Such skeleton may be improved by both automatic filter algorithms (tip removement) or man-machine interactions (gap closing). Doing so, skeletons of proper accuracy have been extracted. For an example the skeleton of figure 9(C) is plotted in figure 11(A). The displacement values have been evaluated giving a standard deviation from a fitted curve of $\sigma_\varphi = 12°$ corresponding to a casual displacement error of $2\sigma_d = 43$ nm. The displacement field calculation proceeds with semiautomatic fringe order asignment and interpolation of broken fringe orders on a regular mesh (32×32 nodal points). The final plotting of the experimental result (1024 points) appears after altogether 2 - 3 min and the pseudo-3D-plot of the displacement field corresponding to the skeleton in figure 11(A) is printed in figure 11(B).

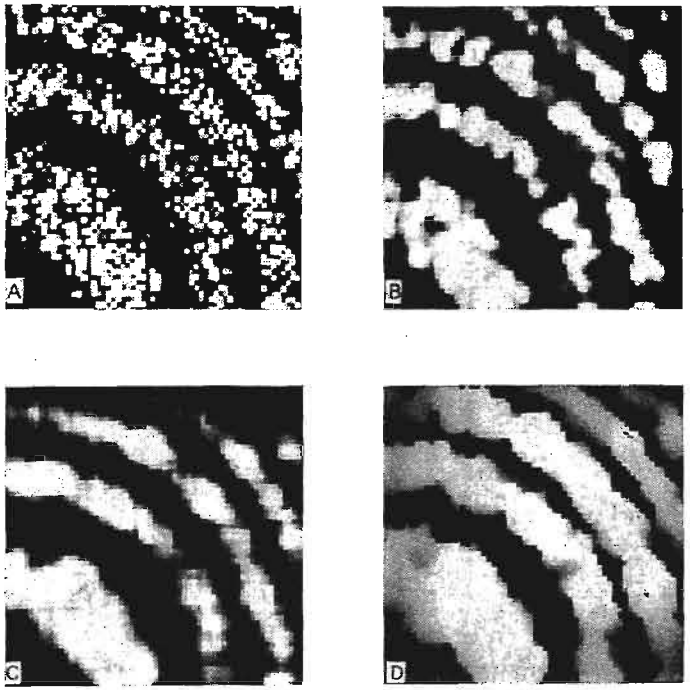

Fig. 8. Correlogram smoothing by different filters

(A) original (part of fig. 4(C), 64 × 64 pixel), (B) 3 × 3 mean filter applied to (A) (0.08 s), (C) 7 × 7 mean filter applied to (A) (0.24 s), (D) four cycles of geometric filter applied (A) (1 min)

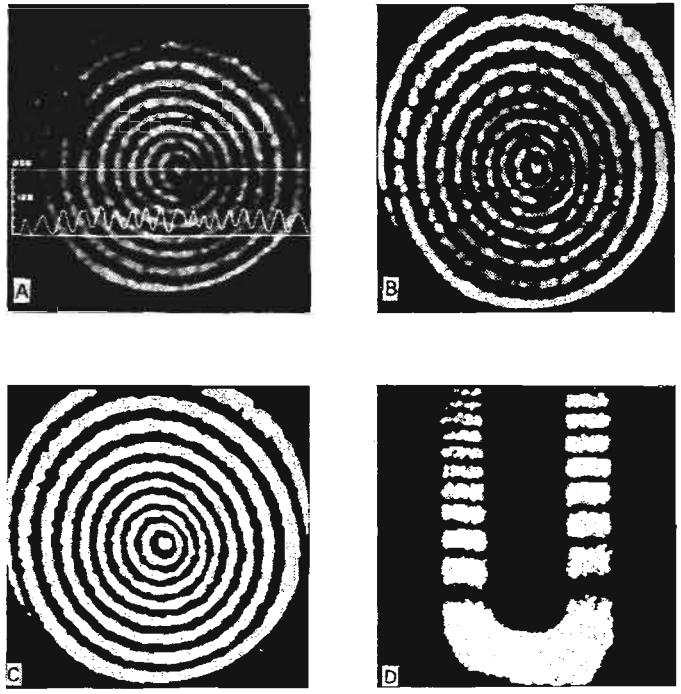

Fig. 9. Demonstration of preprocessing steps

(A) smoothed correlogram, (B) image (A) devided by a „very-low" pass filtered, C) binary image of (B), (D) binary image of the in-plane displacement of a tuning-fork

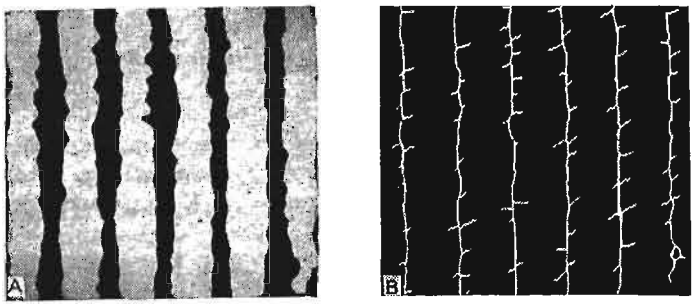

Fig. 10. Skeleton extraction by line thinning
(A) binary image of fig. 7(A), (B) line thinning algorithm apllied to (A)

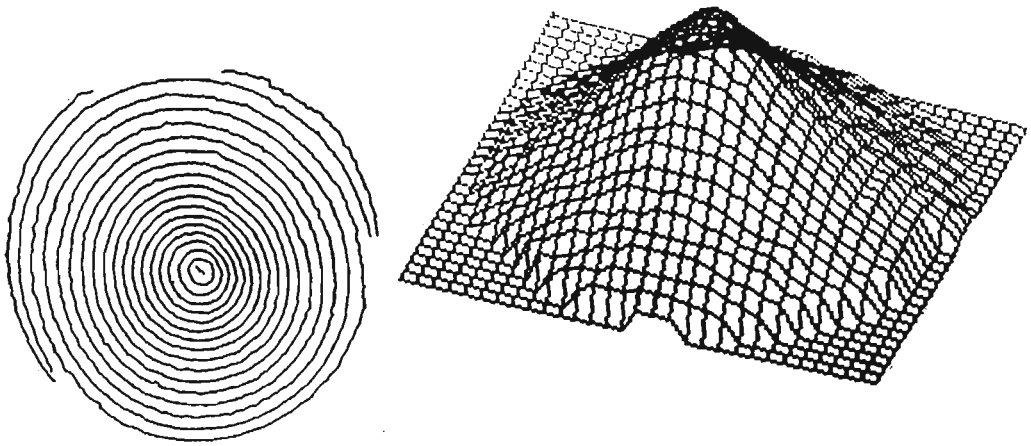

Fig. 11. Skeleton of fig. 9(C) and plotting of the displacement field

6. References

1. H. M. PEDERSEN, Optica Acta, Vol. 29, 105 - 118 (1982)
2. I. YAMAGUSHI, Progr. in Optics, Vol. XXII, 272 - 339 (1985)
3. J. W. GOODMAN, in Laser Speckle and Related Phenomena by J. C. Dainty (ed.), Springer, 1984
4. R. JONES, C. WYKES, *Holographic and Speckle Interferometry*, Cambridge University Press, 1983
5. J. N. BUTTERS, in The Engineering use of coherent Optics by E. R. Robertson (ed.), Cambridge, 1976
6. S. NAKADATE, H. SAITO, Appl. Optics, Vol. 24, 2171 - 80 (1985)
7. O. J. LOKBERG, G. A. SLETTMOEN, Proc. SPIE, Vol. 398, 295 - 9 (1983)
8. K. CREATH, Appl. Optics, Vol. 24, 3053 - 8 (1985)
9. K. CREATH, Topical Meeting on Mach. Vision THB 4/1 - 4 (1985)
10. K. CREATH, G. A. SLETTMOEN, J. Opt. Soc. Am. A Vol. 2, 1629 - 36
11. D. W. ROBINSON, D. C. WILLIAMS, Opt. Commun. Vol. 57, 26 - 30 (1986)
12. R. HÖFLING, W. OSTEN, (to be published in Optica Acta)
13. N. EICHHORN et al., Acta Polytech. Scand. Appl. Phys. Ser. No. PHY 150, 88 - 91 (1985)
14. J. SAEDLER et al., Bild und Ton, Vol. 39, 140 - 4, 165 - 73 (1986)
15. T. R. CRIMMINS, Appl. Optics, Vol. 24, 1439 - 43 (1985)
16. T. R. CRIMMINS, Opt. Engng. Vol. 25, 651 - 4 (1986)

Резюме

КОРРЕЛЯЦИЯ СПЕКЛ-КАРТИН ПРИ ПРИМЕНЕНИИ ЦИФРОВОЙ ОБРАБОТКИ ОБРАЗОВ

В работе представлено спекле интерферометрию при использовании свойств цифровой обработки образов (Digital speckle pattern interferometry). В исследованиях использовано систему ROBOTRON A 6472 с видикон-камерой о 512 × 512 пикселях. Исследовано перемещения в плоскости и перпендикулярные к ней.

Streszczenie

KORELACJA OBRAZÓW PLAMKOWYCH PRZY UŻYCIU TECHNIKI CYFROWEJ

W pracy przedstawiono interferometrię plamkową wykorzystując właściwości cyfrowego przetworzenia obrazów (Digital speckle pattern interferometry). Badania wykonano przy wykorzystaniu systemu ROBOTRON A 6472 wyposażonego w vidicon-kamerę o 512 × 512 pixelach. Badano przemieszczenia w płaszczyźnie i przemieszczenia o kierunku normalnym do płaszczyzny.

Praca wpłynęła do Redakcji dnia 1 czerwca 1987 roku.